REGULATORY INFORMATION DISTRIBUTION SYSTEM (RIDS)

ACCESSION NBR:7904230169 DOC.DATE: 79/04/16 NOTARIZED: NO DOCKET #
FACIL:50-315 DONALD C. COOK NUCLEAR POWER PLANT, UNIT 1, INDIANA & 05000315
50-316 DONALD C. COOK NUCLEAR POWER PLANT, UNIT 2, INDIANA & 05000316
AUTH.NAME AUTHOR AFFILIATION
DOLAN,J.E. INDIANA & MICHIGAN POWER CO.
RECIP.NAME RECIPIENT AFFILIATION
DENTON,H.R. OFFICE OF NUCLEAR REACTOR REGULATION

SUBJECT: FORWARDS ADDL INFO RE SPENT FUEL STORAGE CAPACITY EXPANSION PROGRAM.ENCL INFO INCLUDES DETAILS OF STRUCTURAL ANALYSIS, & REVISIONS TO GENERAL DESCRIPTION OF NEW SPENT FUEL RACKS & TO THERMAL ANALYSIS.

DISTRIBUTION CODE: A001S COPIES RECEIVED:LTR 1 ENCL 1 SIZE: 35
TITLE: GENERAL DISTRIBUTION FOR AFTER ISSUANCE OF OPERATING LIC.

NOTES: I&E - 3 CYS ALL MATL.

	RECIPIENT ID CODE/NAME	COPIES LTTR	COPIES ENCL	RECIPIENT ID CODE/NAME	COPIES LTTR	COPIES ENCL
ACTION:	05 BC ORB #1	7	7			
INTERNAL:	01 REG FILE	1	1	02 NRC PDR	1	1
	12 I&E	2	2	14 TA/EDO	1	1
	15 CORE PERF BR	1	1	16 AD SYS/PROJ	1	1
	17 ENGR BR	1	1	18 REAC SFTY BR	1	1
	19 PLANT SYS BR	1	1	20 EEB	1	1
	21 EFLT TRT SYS	1	1	22 BRINKMAN	1	1
EXTERNAL:	03 LPDR	1	1	04 NSIC	1	1
	23 ACRS	16	16			

APR 24 1979

TOTAL NUMBER OF COPIES REQUIRED: LTTR 38 ENCL 38

MA 4
GD

INDIANA & MICHIGAN POWER COMPANY
P. O. BOX 18
BOWLING GREEN STATION
NEW YORK, N. Y. 10004

April 16, 1979
AEP:NRC:00169

Donald C. Cook Nuclear Plant Units No. 1 and 2
Docket Nos. 50-315 and 50-316
License Nos. DPR-58 and DPR-74
Spent Fuel Storage Capacity Expansion Program-Structural Analysis

Mr. Harold R. Denton, Director
Office of Nuclear Reactor Regulation
U.S. Nuclear Regulatory Commission
Washington, D.C. 20555

Dear Mr. Denton:

Please find attached additional information on the Spent Fuel Storage capacity expansion program for the Donald C. Cook Nuclear Plant. A brief description of each attachment follows:

Attachment No. 1 presents the details of the required structural analysis performed by the Exxon Nuclear Company for the new spent fuel racks and replaces the originally submitted sections 3.6 and 3.7 of Reference (1). This analysis completes our submittal describing the spent fuel storage capacity expansion program at the Donald C.Cook Plant.

Attachment No. 2 includes revisions to the general description of the new spent fuel racks given as part of reference (1).

Attachment No. 3 includes revisions to the thermal analysis previously submitted in reference (2).

A001
S/1

The fee for processing this and the previous submittals was remitted to the Nuclear Regulatory Commission on December 21, 1978, reference (3).

Very truly yours,

John E. Dolan
Vice President

JED:em

Sworn and subscribed to before me
this 16th day of April, 1979 in
New York County, New York

Notary Public

KATHLEEN BARRY
NOTARY PUBLIC, State of New York
No. 41-4606792
Qualified in Queens County
Certificate filed in New York County
Commission Expires March 30, 1981

REFERENCES:
(1) Letter AEP:NRC:00105 dated November 22, 1978
(2) Letter AEP:NRC:00116 dated January 22, 1979
(3) Letter AEP:NRC:00118 dated December 21, 1978

cc: R. C. Callen
G. Charnoff
D. V. Shaller - Bridgman
R. W. Jurgensen
P. W. Steketee
R. J. Vollen
R. Walsh

ATTACHMENT 1

3.6 MECHANICAL CONSIDERATIONS

3.6.1 Design Criteria

Structural design criteria for spent fuel storage racks have been developed to assure conformance with recognized codes and applicable regulatory guides (current revisions) as follows:

1. The fuel storage rack design is based on the requirements of the ASME Boiler and Pressure Vessel Code, Section III, Division I, Subsection NF, Class III Supports.

2. Regulatory Guide 1.13 - The design conforms with the stated provisions for spent fuel storage equipment.

3. Regulatory Guide 1.29 - The spent fuel storage racks are designed as Seismic Category I Structures.

4. Regulatory Guide 1.92 - Seismic load combinations of vibrational modes and three orthogonal component motions (two horizontal and one vertical) are in accordance with the provisions of the Regulatory Guide.

5. Regulatory Guide 1.124 - The fuel storage rack design is in accordance with the provisions of Paragraphs C.2, C.3 and C.4 of the Regulatory Guide.

3.6.2 Design Loads and Load Combinations

The loads (defined below) are combined and compared with section strengths in accordance with Table 3.6.1, which is compiled from the requirements of the NRC Position Paper entitled, "Review and Acceptance of Spent Fuel Storage and Handling Applications"; the NRC Standard Review Plan Section 3.8.4 for Seismic Category I Structures Outside Containment; and ASME Section III NF-3400:

Dead Load

D = Dead load of fuel module structure and stored fuel.

Live Loads

L_a = Load from force of lowering a fuel assembly at maximum crane speed.

L_b = Crane uplift force.

L_c = Load from accidental release of a fuel assembly while handling.

Thermal Loads

T_o = Thermal loads during maximum normal conditions.

T_a = Thermal loads resulting from maximum pool temperature during boiling at the pool surface.

Seismic Loads

E = Loads generated by Operating Basis Earthquake (OBE).

E = Loads generated by Safe Shutdown Earthquake (SSE).

TABLE 3.6.1

LOAD COMBINATIONS AND ACCEPTANCE CRITERIA

Load Combination	Linear Member[1] Acceptance Limit	Plate Member[1] Acceptance Limit
$D + E$	Per NF-3231.1a	Per NF-3321.2(a)[2]
$D + L_a$	Per NF-3231.1a	Per NF-3321.2(a)[2]
$D + L_b$	Per NF-3231.1a	Per NF-3321.2(a)[2]
$D + L_a + T_o$	The lesser of 2 Sy and Su stress range.	Per NF-3321.2(b)[2]
$D + L_b + T_o$	"	Per NF-3321.2(b)[2]
$D + L_c + T_o$	"	Per NF-3321.2(c)
$D + T_o + E$	"	Per NF-3321.2(b)[2]
$D + T_a + E$	"	Per NF-3321.2(c)
$D + T_a + E$ [3]	Faulted condition limits of NF-3231.1c	Per NF-3321.2(d)

Note 1: The provisions of NF-3231.1 and NF-3321.2 shall be amended by the requirements of the paragraphs c.2, 3, and 4 of the Regulatory Guide 1.124 entitled "Design Limits and Load Combinations for Class 1 Linear-Type Component Supports."

Note 2: Factors of safety against buckling shall be consistent with Appendix XVII-2213.2.

Note 3: Self-limiting stresses due to T_a may be neglected.

3.6.3 Material Properties and Allowable Stresses

The material properties for structural components of the fuel racks used in the analysis were taken from Appendix I of Section III of the ASME Code. The values used in the analysis for Type 304 stainless steel as interpolated from the ASME Code (minimum specified strength values) are as follows:

Yield Strength

Sy = 27.5 Ksi at 150°F

Sy = 24.0 Ksi at 240°F

Ultimate Strength

Su = 73.5 Ksi at 150°F

Su = 69.0 Ksi at 240°F

Modulus of Elasticity

E = 28,000 Ksi

Coefficient of Thermal Expansion

a = 0.0000095 in/in/°F

The material properties at 150°F were used for all load cases at normal operating temperatures (T_o) and 240°F properties were used for the load cases at maximum temperature (T_a).

Appropriate allowable stresses were derived from the above for the tension, compression and shear (including buckling instability in accordance with the provisions of Paragraph 3.6.2.

Type 304 stainless steel is the only structural material used in the fuel storage racks. The only other material used is the Boral™ neutron poison material which is supported in the storage cells so that it will be non-load bearing. No credit was taken for any strength contributed by the Boral™ in the structural analysis.

3.6.4 Seismic Analyses

A combination of time history and modal response spectrum analyses were performed. The ANSYS[10] computer program was used for the time history analyses, and a Boeing Computer Systems modified version of the SAP-IV[9] computer program was used for modal response spectrum and static analyses.

3.6.4.1 SAP-IV Elastic Analysis

The SAP-IV computer program was used for linear elastic static and dynamic analysis of the fuel storage rack structure. The analytical model is sufficiently detailed to allow determination of static and dynamic loads on all rack members.

The total mass of the water enclosed in the spent fuel storage rack is lumped together with the masses of the fuel assembly and the rack structure in the horizontal direction in the lumped-parameter SAP-IV model. Due to the 6-inch diameter flow holes provided in the bottom of each storage cell for coolant flow, vertical motion of the water was not considered to be restrained, and no vertical virtual mass was added.

Static analysis output consists of member loads and deflections. Dynamic analysis output includes frequencies, mode shapes, participation factors and member loads.

Detailed structural analysis for static and dynamic loads has been completed. Figure 3.6.1 shows the SAP-IV computer analysis model. The analytical model is for a complete rack structure and comprises 251 nodes and 460 structural elements. The model comprises beam, truss and membrane elements to represent the various rack members.

Static and seismic loads obtained from the SAP-IV model were combined together and with other loads (per Section 3.6.2) to calculate stresses in the structural members. Horizontal and vertical seismic loads were increased by factors to allow for impact of the fuel assemblies against the fuel storage cells and fuel storage rack rocking and sliding motion. Details of the nonlinear analysis performed to develop these impact factors are given below. The calculated stresses were then compared with the applicable allowable stresses to confirm the structural adequacy.

The seismic response spectra used for analysis of the fuel storage racks were the floor level spectra developed from the seismic analysis of the auxiliary building, at the elevation of the spent fuel storage pool floor. The response spectra used in the analysis conform to those submitted to the NRC in Attachment IV of the response to the Seismic Qualification Review Team dated November 17, 1977 Docket No. 50-316, CPPR No. 61.

Seismic excitations along the three orthogonal directions were combined by the SRSS method in accordance with the requirements Regulatory Guide 1.92.

Two percent (2%) damping was used for both OBE and SSE loading consistent with the values used in the FSAR. Regulatory Guide 1.61 allows up to 2% damping for the OBE and 4% damping for the SSE for welded steel structures. No credit was taken for additional damping due to submergence in water.

3.6.4.2 ANSYS Time History Analysis

Time history analyses were performed to account for the effects of the clearance gap between the storage cells and the fuel assemblies contained therein plus the effects of a fuel storage rack rocking and sliding on the pool floor.

The simplified dynamic model used in the ANSYS analysis is shown in Figure 3.6.2. In this model, all of the fuel assemblies are conservatively assumed to be moving in phase with each other and are, therefore, lumped together, as also are the fuel cells. The fuel assemblies are represented by nodes 11 through 15 and the fuel cells are represented by nodes 4 through 8 and 16 through 19 to account for fuel assemblies rattling within the fuel cells. Fuel assembly mass, stiffness and damping values used in the analysis were taken from experimental results for D. C. Cook reload fuel supplied by Exxon Nuclear Company.

In the actual rack, the fuel cells are welded to the rack structure at the top and bottom only. In the ANSYS model, the rack is, therefore, represented as a rigid inverted Tee with no mass (Nodes 1-10-3 and 10-2-9) supporting the fuel cells horizontally at the top and bottom with springs K_T and K_B and vertically with spring K_V. The stiffness of springs K_T and K_B were selected to duplicate the frequency and mode shape of the primary horizontal mode of the complete rack assembly as determined from the SAP-IV detailed elastic model. The stiffness of the vertical support spring K_V was selected to duplicate the frequency of the primary vertical mode.

Added hydrodynamic mass was treated in the same manner as with the SAP-IV model, i.e. it was included in the horizontal direction but not in the vertical direction. The mass of the rack structure was included at Nodes 4 and 8. Sliding gap elements are provided between Nodes 1 and 20 and Nodes 3 and 21 to permit both rocking and sliding of the complete rack assembly. Analyses were performed for both minimum and maximum friction coefficient values. The values used were respectively 0.30 and 0.75 and are taken from the results of experimental work reported in References (11) and (12). The values used are based on statistical analysis of the experimental results and provide at least a 95% confidence level that the actual friction coefficient at any contact point will not fall outside the range of the values used. Impact between adjacent racks was considered by providing gap elements between nodes 8 and 22 and nodes 19 and 23. The initial gap in these elements was set equal to half the gap between adjacent racks, and conservatively assumes that racks could be moving out of phase with each other.

The model was subjected to simultaneous, statistically independent horizontal and vertical time histories at the pool floor; i.e. Nodes 20 and 21. These were artificially generated time histories whose response spectra enveloped the floor level response spectra for the floor of the fuel storage pool.

The results from the nonlinear time history analysis were compared with the results of simplified elastic time history analyses to develop impact factors for use in the detailed stress analysis. This simplified elastic time history analysis was performed by closing all the fuel cell to fuel gaps and by fixing the rack feet sliding gap elements in the model shown in Figure 3.6.2.

3.6.5 Dropped Fuel Assembly Accident

An evaluation of the effects of a postulated dropped fuel assembly accident has been performed to confirm that there would be no effect on the spacing of fuel assemblies stored in the racks. The method of design and analysis was identical to that submitted by Public Service Electric and Gas Company in it's letter dated November 18, 1977 and subsequent submittals and as approved by the NRC in its Safety Evaluation Report for the Salem Station Unit No. 1 Spent Fuel Rack Modification dated January 15, 1979.

3.6.6 Results

Structural Analysis

Computer plots of the primary vibrational mode shape in the horizontal and vertical directions are presented in

Figures 3.6.3, 3.6.4 and 3.6.5. The calculated natural frequencies and participation factors are given in Table 3.6.2.

The limiting load combinations and stress values for the rack members are presented in Table 3.6.3.

Time History Analyses

The results obtained from the time history analyses are as follows:

(a) The maximum horizontal motion at the top of a fully loaded rack resulting primarily from sliding motion with a friction coefficient of 0.3 is 0.46 inches under SSE loading conditions.

(b) The maximum horizontal motion at the top of a fully loaded rack, resulting primarily from rocking, with a friction coefficient of 0.75 is 0.64 inches under SSE loading conditions.

(c) The maximum horizontal motion of a worst case partially loaded rack, primarily resulting from rocking, with a friction coefficient of 0.75 is 3.29 inches under SSE loading conditions. This is the worst case loading condition for overturning and shows that there is a large factor of safety against rack overturning. This case could only occur for a peripheral rack rocking away from the center of the array. A worst case partially loaded rack within the array will impact against adjacent racks and the resulting impact loads have been included in the structural analysis of the rack members.

(d) The elastic lumped parameter analysis loads are increased by impact factors of 1.54 and 1.94 for SEE and OBE loads, respectively. Consequently, the loads developed from the SAP-IV elastic analysis were increased by these factors for comparison against the allowable stresses.

(e) The maximum loads on the fuel assembly from the nonlinear seismic impact analysis with the assembly modeled with three equally spaced spacer grids, are 840 lbs on the upper end fitting, 800 lbs, 1120 lbs and 520 lbs, respectively on the top, middle and bottom spacer grids, and no load on the bottom end fitting. A transverse compression test was performed as part of testing on the stainless steel clad Boral fuel cell. This test showed that the cell could elastically resist a uniform load of up to 105 lbs/in^2 against the side of the cell. Therefore, for the maximum impact load against the side of the cell, only a 1.3 inch length of cell would be required to resist this load, which is much less than the area impacted by the fuel bundle. At the location of the fuel assembly upper end fittings, additional conservatism is provided by the fact that the fuel cells are supported by the intercell spacer grid bars.

Dropped Fuel Assembly Accident

Compression tests were performed on 2-ft long sections of the Boral poison spent fuel cell together with the flared lead-in section to determine the load-deflection characteristics of the cell. Two (2) cases were considered. The first case is that of an assembly falling vertically directly on one cell but rotated 45° such that the corners of the assembly hit the sides of the cell in a diamond pattern. This case produces maximum force and deflection of an individual cell. The second case is that of an assembly falling vertically at the center of a group of four (4) cells, resulting in a maximum force applied to the rack structure.

Each of the specimens was made of a 2 foot long section of the Boral poison spent fuel cell together with the flared insertion guide attached at the top. A steel bearing plate was attached to the bottom for support. The load was applied by a thick square steel loading plant mounted on the load head of a 120 kip static test machine. The plate, representing the bottom of a fuel assembly, contacted the top of the insertion guide in a manner which represented the alignment and orientation of the fuel assembly with respect to the fuel cell at the assumed time of impact. An increasing load was slowly applied and the load-deflection recorded until the insertion guide was significantly deformed. In each of the two (2) tests, the structure deformed elastically up to the onset of localized inelastic buckling. In the first case where

the four (4) corners of the loading plate contact the mid-length of the four (4) sides of the cell, initial inelastic deformation occurred at a load of 4,500 lbs. The maximum load of 25,000 lbs occurred at a deflection of 2.5 inches. In the second case where the loading plate is centered on a group of four (4) fuel cells, initial inelastic deformation occurred at a load of 5,000 lbs for the one cell tested. The maximum load of 10,000 lbs occurred at a deflection of 0.8 inches. In both cases, local crushing of the cell was limited to the upper 7 inches of the insertion guide.

The mechanical properties of Type 304 stainless steel have been shown to be relatively insensitive to strain rate over a wide range. It is, therefore, concluded that the static load tests, described above, adequately represent the response to fuel cell impact at the low velocities involved (approximately 8 ft per second).

The experimentally developed load-deflection curves were used to calculate the peak force and deflection resulting from the energy of a dropped assembly. The maximum drop height is 15 inches from the top of the fuel cells, since the fuel assemblies will not be moved over the fuel storage racks at a higher elevation. The maximum kinetic energy at the point of impact is 2,020 ft-lbs. For the first case (diamond pattern) the maximum force, on the impacted cell, is 25,000 lbs and the maximum deflection is 2.5 inches. For the second case, the maximum force on

each of the four (4) impacted cells is 10,000 lbs and the maximum deflection is 0.8 inches. In both cases, local crushing of the cell is limited to the upper 7 inches of the lead-in section, above the rack module upper grid structure and above stored fuel assemblies.

In the case where the fuel assembly is dropped inside the storage cell, the fuel assembly would impact the 1/4 inch base plate at the bottom of the rack module. The impact energy will be absorbed primarily by bending deformation of the 1/4 inch base plate and a small amount of bending distortion of the base assembly beam members. The total distortion of the base plate was conservatively calculated to be approximately 1 inch. The spacing of adjacent stored fuel assemblies will not be affected.

The effects of a dropped assembly accident in which the assembly rotates as it drops, was also evaluated. In this case, the assembly impacts a row of storage cells and comes to rest laying on top of the rack modules. The maximum kinetic energy of impact on one cell is conservatively calculated to be 1,500 ft-lbs resulting in lower loads than the simple vertical drop case discussed above.

The dynamic response of the rack structure to the impulsive type loading of the fuel bundle drop accidents described above has been evaluated and the resulting rack member stresses compared against the allowables. The results of these analyses show that:

1) Inelastic deformations are limited to the immediate area(s) of assembly impact.

2) All other rack member stresses are within the limits specified in Section 3.6.2.

3.6.7 Fuel Storage Pool Hydrodynamic Effects

The array of fuel storage racks are located within 11-inch or less of the fuel storage pool walls on the North, South and West walls of the fuel storage pool. Any effects of this small mass of water on the vibrational response or stress in the racks were, therefore, considered to be insignificant. At the East end of pool in the cask area, there is a 12 ft clearance between the fuel storage racks and the pool wall. The seismic effects on the racks of the water in this area were analyzed in accordance with the methods given in Reference 13. The added hydrodynamic loads increase the horizontal seismic loads in the East-West direction by 8%. This results in a substantially smaller percentage increase in stresses when three axes simultaneous seismic loads are combined with the dead weight loads on the rack structure.

3.6.8 Fabrication and Installation

The spent fuel storage rack modules are in conformance with the materials, fabrication, installation and examination criteria of the 1977 Edition of the ASME Code, Section III, Subsection NF Articles NF-2000, NF-4000, and NF-5000, respectively, except as specifically noted below.

The fuel storage modules are not certified or stamped as Section III components; therefore, the documentation, certification and programs which are specifically concerned with production of Code certified components have been replaced with Exxon Nuclear Company's QA/QC program, which is in compliance with ANSI N45.2 and 10 CFR 50, Appendix B.

Exxon Nuclear does not require compliance with the material traceability requirements of NF-4122. The fabricator is required to demonstrate a material control program which will insure that only certified material is used in the storage module. The only exception to this rule is in the use of neutron poison materials, which are required to be in compliance with NF-4122.

TABLE 3.6.2

NATURAL FREQUENCIES AND MODAL PARTICIPATION FACTORS

Mode #	Frequency (Hz)	Participation Factor X	Y	Z	Notes
1	7.19	0.52	0.12	0.02	
2	7.46	21.34	0.56	0.02	Primary X-Mode
3	7.63	0.57	20.87	0.01	Primary Y-Mode
4	7.91	0.31	0.17	0.02	
5	10.45	0.00	0.01	0.01	
6	10.70	2.32	0.04	0.01	
7	10.72	0.04	2.53	0.01	
8	10.73	0.11	0.11	0.02	
9	11.23	0.01	0.01	0.02	
10	11.34	0.20	0.01	0.02	
11	11.35	0.03	0.11	0.02	
12	11.37	0.01	0.00	0.02	
13	11.44	0.00	0.00	0.00	
14	11.50	0.21	0.00	0.03	
15	11.51	0.02	0.01	0.01	
16	11.53	0.00	0.20	0.01	
17	11.53	0.01	0.01	0.07	
18	11.57	0.00	0.01	0.00	
19	11.59	0.01	0.11	0.01	
20	11.78	0.01	0.00	0.02	
21	11.82	0.00	0.00	0.01	
22	11.85	0.01	0.00	0.01	
23	11.85	0.01	0.00	0.05	
24	11.86	0.00	0.01	0.01	
25	16.26	0.25	2.62	0.08	
26	16.37	2.85	0.27	0.01	
27	16.43	0.35	0.22	0.05	
28	18.06	0.00	0.00	0.02	
29	22.52	5.93	0.01	0.12	
30	22.82	0.00	4.73	0.00	

TABLE 3.6.2 (Continued)

Mode #	Frequency (Hz)	Participation Factor X	Y	Z	Notes
31	23.28	0.03	0.01	0.13	
32	26.20	1.31	0.07	0.34	
33	26.36	6.14	0.10	0.24	
34	27.05	0.19	5.41	0.19	
35	30.29	2.83	0.12	0.96	
36	30.77	0.21	0.18	2.16	
37	31.10	0.20	0.39	19.12	Primary Z-Mode

TABLE 3.6.3

COMPARISON OF MOST LIMITING STRESSES
AND ALLOWABLE STRESSES ON STRUCTURAL MEMBERS

Structural Member	Most Limiting Load Combination	Type Of Stress	Most Limiting Combined Stress Ratio	Allowable Limit
Upper Grid Bars	D + E	Bending	1.01	1.0
Top Peripheral Beam	D + E	Bending + Axial	0.55	1.0
Mid-Height Peripheral Beam	D + E	Bending + Axial	0.07	1.0
Vertical Corner Angles	$D + T_a + E'$	Bending + Axial	0.49	1.0
Base Angles	D + E	Bending + Axial	0.80	1.0
Outer Base Channel	$D + T_a + E'$	Bending + Axial	0.96	1.0
Center Base Channel	$D + T_a + E'$	Bending + Axial	1.0	1.0
Outer Shear Diaphragms	$D + T_a + E'$	Shear + Compression Buckling	0.99	1.0
Internal Shear Diaphragm	$D + T_a + E'$	Shear + Compression Buckling	0.92	1.0
Fuel Cells	$D + T_a + E'$	Bending + Axial	0.82	1.0
Feet Brackets	$D + T_a + E'$	Bending	1.0	1.0
Screw Feet	$D + T_a + E'$	Bending + Axial	0.89	1.0

Figure 3.6.1
SPENT FUEL STORAGE RACK
SAP-IV SEISMIC MODEL

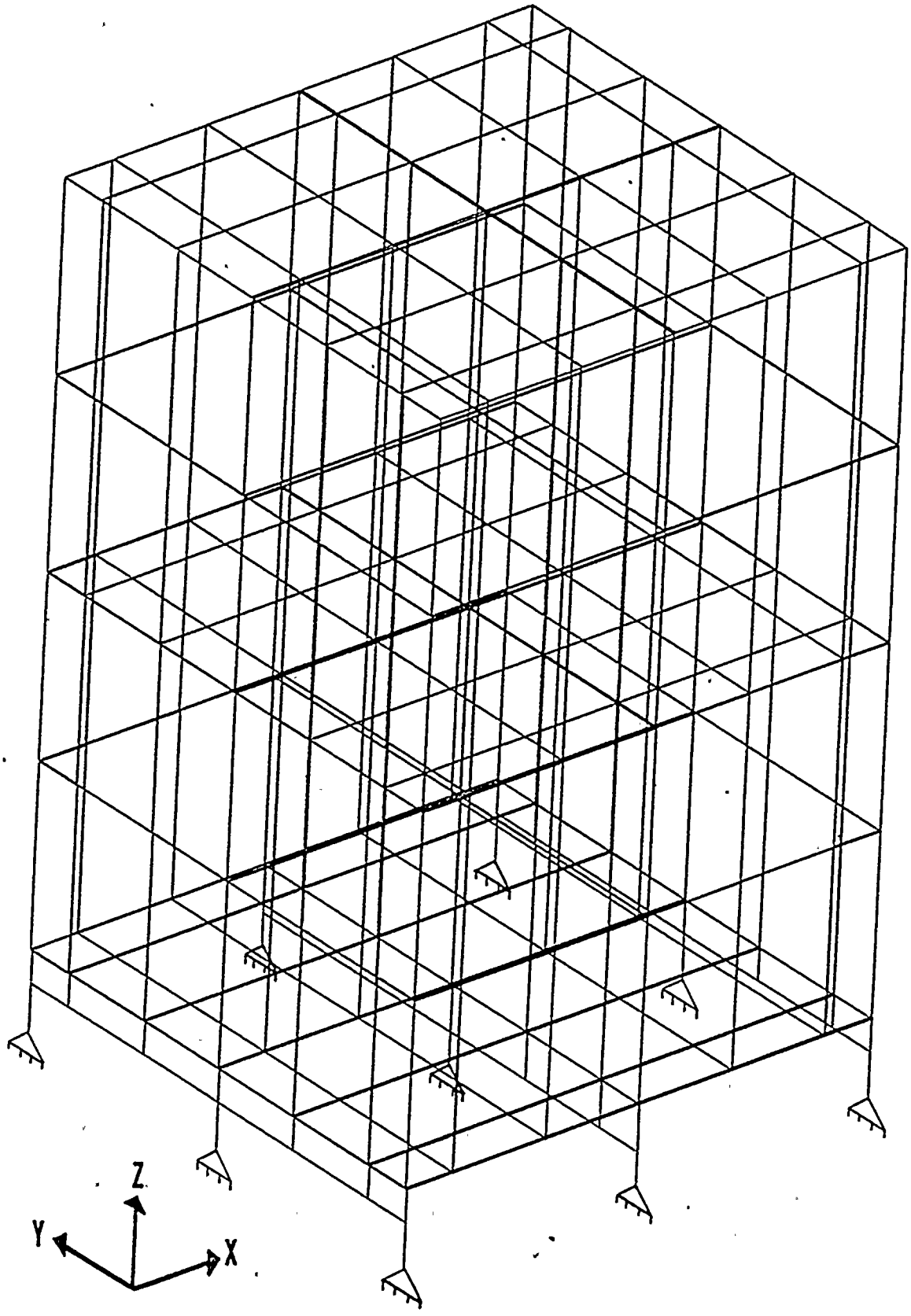

Figure 3.6.2
SINGLE STORAGE RACK
NON-LINEAR MODEL

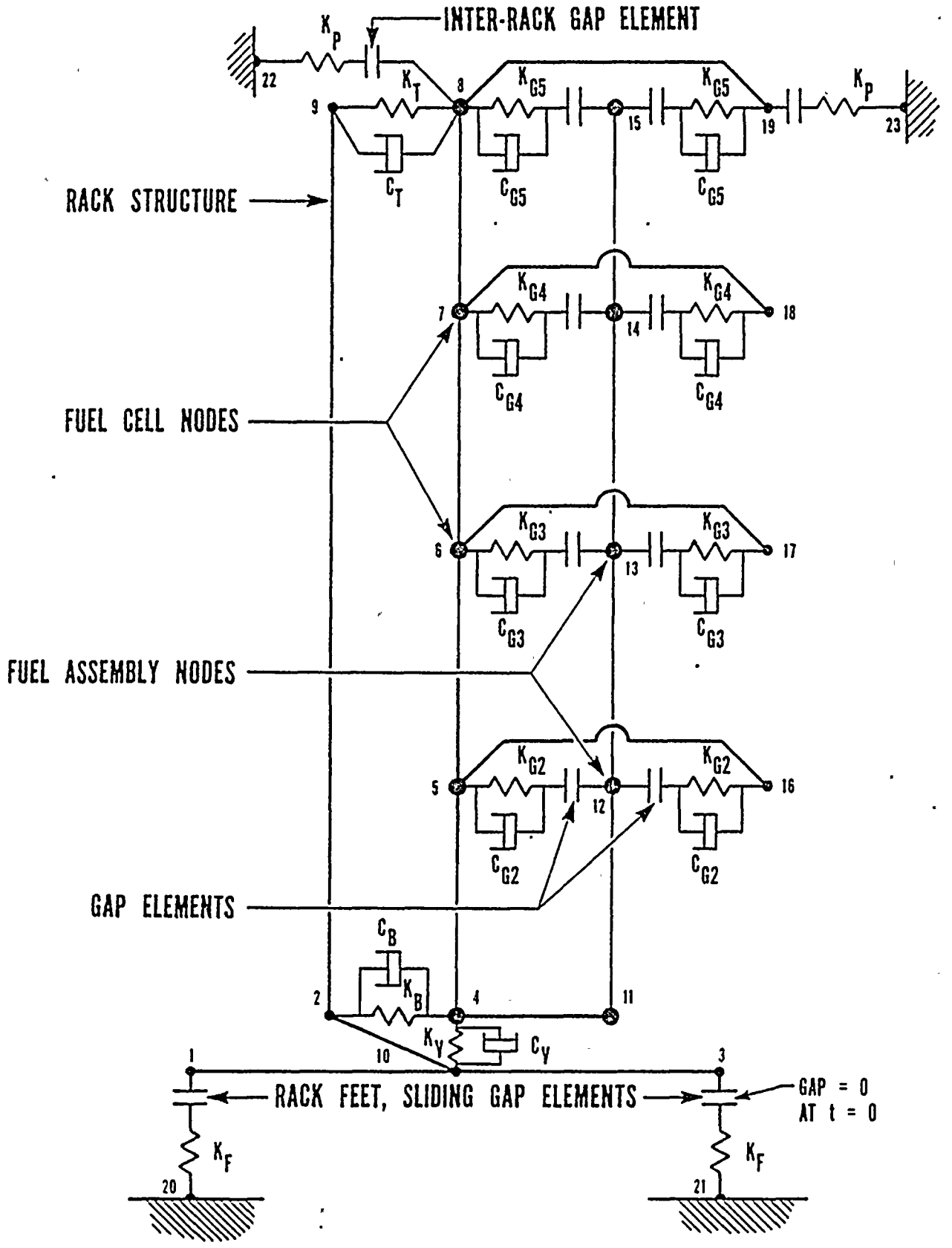

23 MARCH 1979 sh

Figure 3.6.3
MODE SHAPE 2
(Primary X Mode)

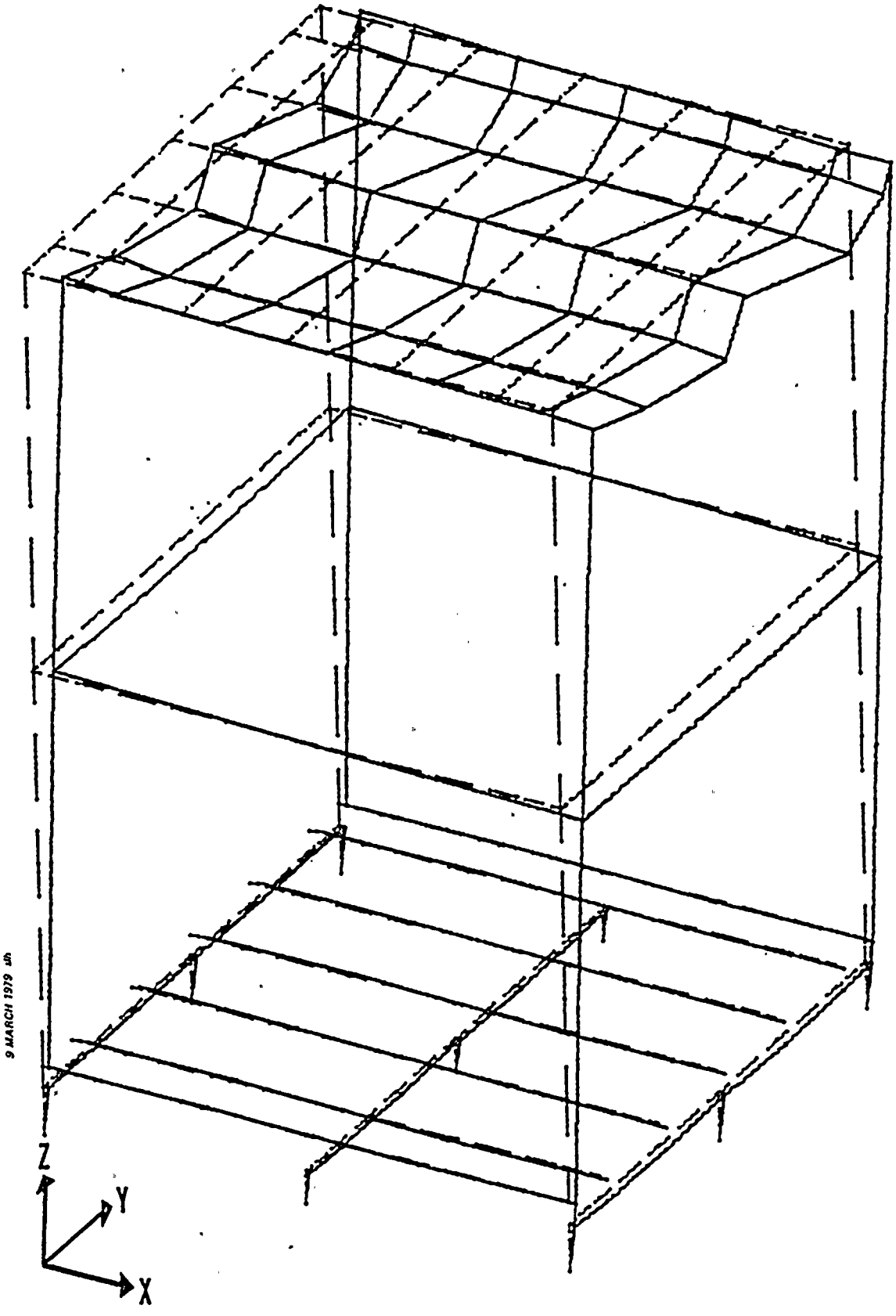

Figure 3.6.4
MODE SHAPE 3
(Primary Y Mode)

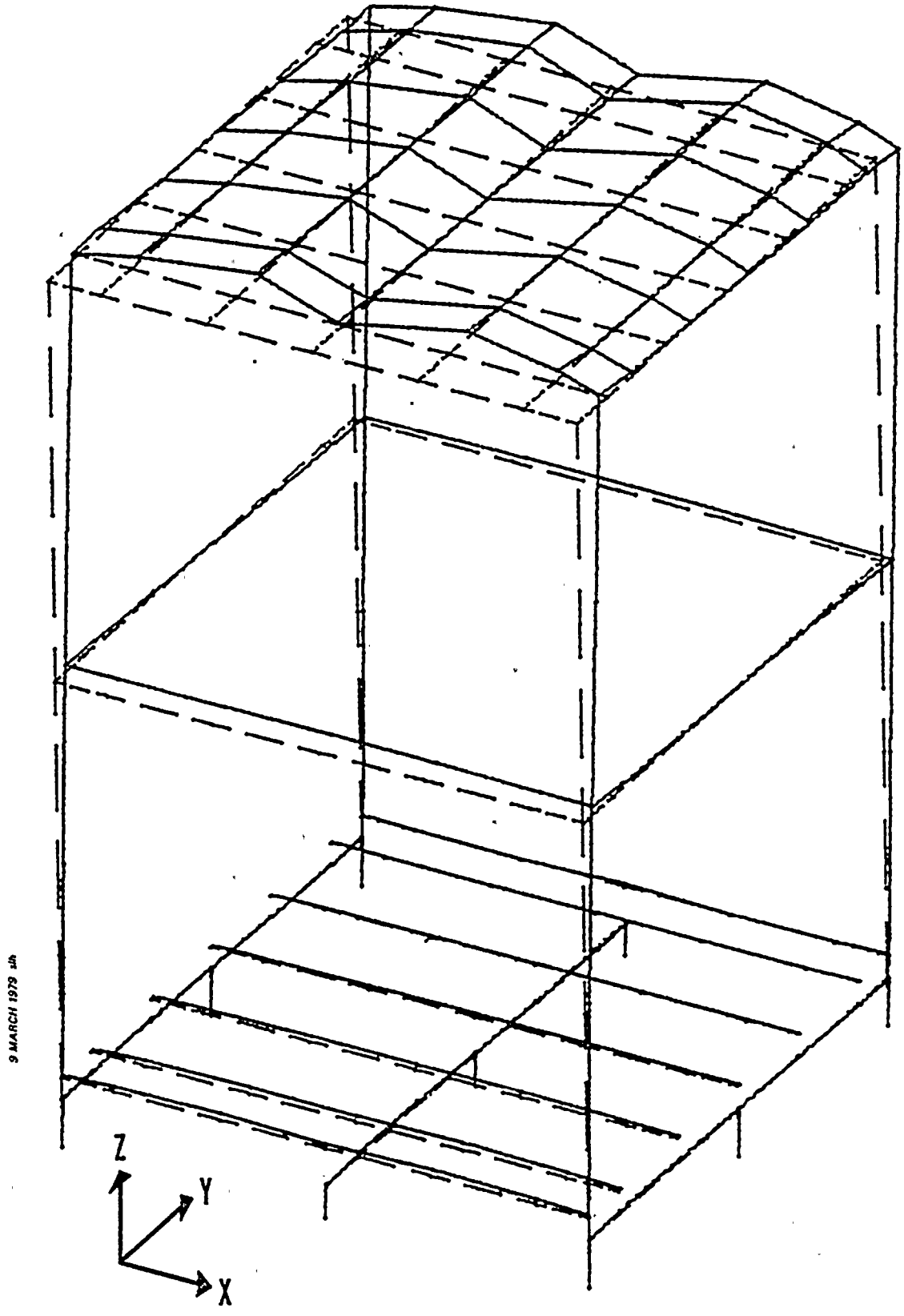

Figure 3.6.5
MODE SHAPE 37
(Primary Z Mode)

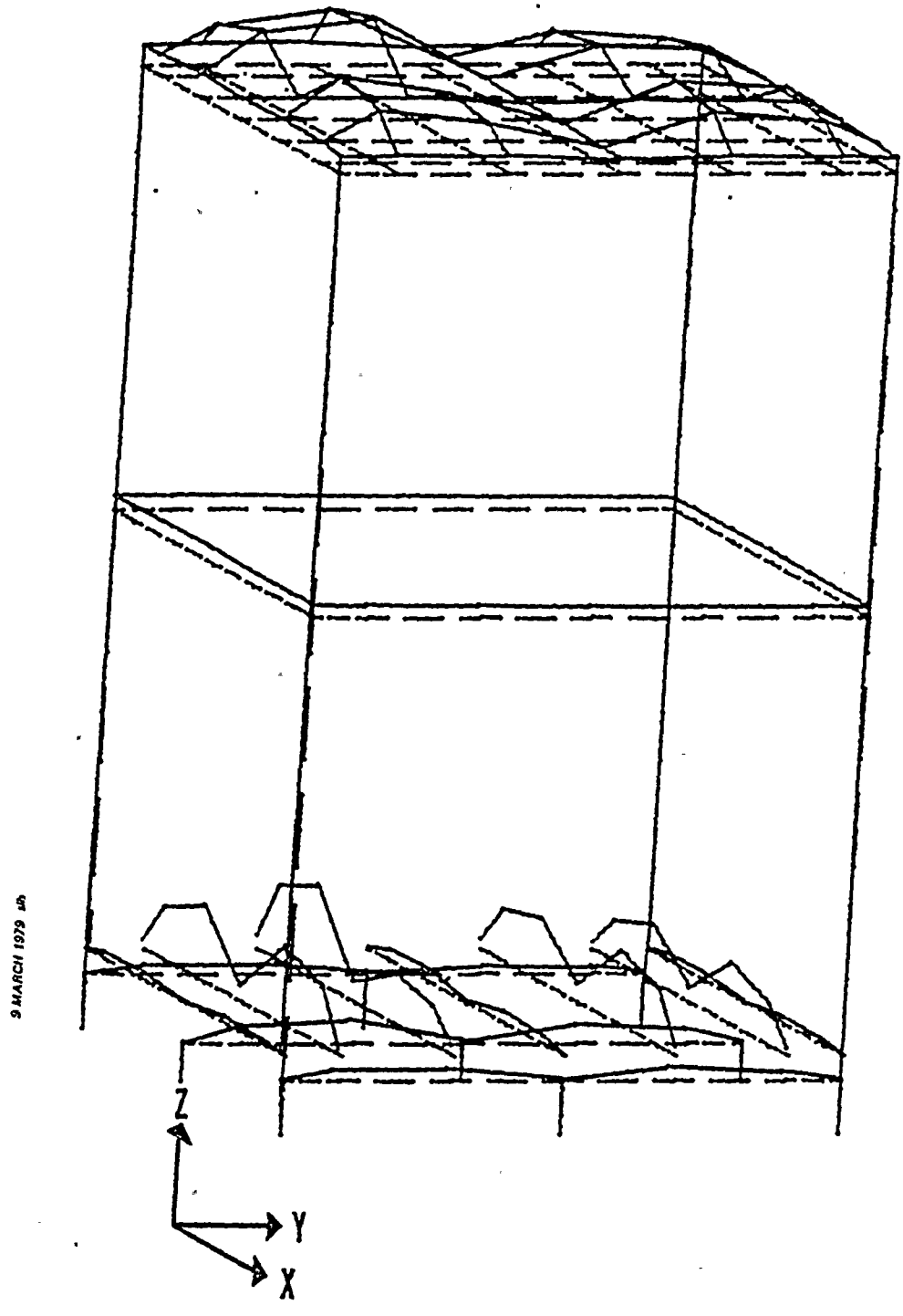

3.7 References

(1) L. M. Petrie and N. F. Cross, "KENO IV: An Improved Monte Carlo Criticality Program," ORNL-4938, Oak Ridge National Laboratory (November 1975).

(2) N. M. Greene, et al, "AMPX - A Modular Code System for Generating Coupled Multigroup Neutron-Gamma Libraries from ENDF/B," ORNL-TM-3706, Oak Ridge National Laboratory (March 1976).

(3) W. W. Porath, "CCELL Users Guide," BNW/JN-86, Pacific Northwest Laboratories (February 1972).

(4) G. E. Whitesides and N. F. Cross, "KENO - A Multigroup Monte Carlo Criticality Program," CTC-5, Union Carbide Corporation Nuclear Division (September 1969).

(5) V. E. Grob, et al, "Multi-Region Reactor Lattice Studies Results of Critical Experiments in Loose Lattices of UO_2 Rods in H_2O," WCAP-1412, Westinghouse Electric Corporation (1960).

(6) K. D. Lathrop, "DTF-IV - A FORTRAN-IV Program for Solving the Multigroup Transport Equation with Anisotropic Scattering," LA-3373, Los Alamos Scientific Laboratory (July 1965).

(7) Information obtained via personal communication with E. B. Johnson and G. E. Whitesides, Oak Ridge National Laboratory, Oak Ridge, Tennessee (September 1976).

(8) S. R. Bierman, E. D. Clayton and B. M. Durst, "Critical Separation Between Subcritical Clusters of 2.35 Wt.% U-235 Enriched UO_2 Rods in Water with Fixed Neutron Poisons," PNL-2438, Pacific Northwest Laboratories (October 1977).

9. SAP-IV, "A Structural Analysis Program for Static and Dynamic Response of Linear Systems", K. J. Bathe, E. L. Wilson, F. E. Peterson; Earthquake Engineering Research Center Report No. 73-11, Revised April 1976.

10. ANSYS, Engineering Analysis System Users Manual, Swanson Analysis Systems, Inc., Houston, Pa., March 1, 1975.

11. General Electric Report No. 60GL20, "Investigation of the Sliding Behavior of a Number of Alloys Under Dry and Water Lubricated Conditions," R. E. Lee, Jr., January 22, 1960.

12. Friction Coefficients of Water-Lubricated Stainless Steels For a Spent Fuel Rack Facility," Prof. Ernest Rabinowicz, MIT, November 5, 1976, performed for the Boston Edison Company.

13. TID-7024, Nuclear Reactors and Earthquakes, August 1963.

ATTACHMENT 2

Insert the attached page 2 and Figure 1.2 and delete the similarly numbered ones in Attachment 1 to our transmittal No. AEP:NRC: 00105, dated November 22, 1978.

The replacement spent fuel storage racks are to be fabricated primarily from type 304 stainless steel. The individual fuel assemblies will be stored in square fuel storage cells fabricated from stainless steel-clad Boral* material. The high density (poison) spent fuel module construction is essentially a replica of the design used in the replacement racks for the Salem Nuclear Generating Station, which the Commission approved in the Safety Evaluation Report dated 1-15-79. . The module is shown in Figure 1-2.

The design utilizes a stiffened module base and an upper box structure consisting of plate diaphragms and a top grid. The vertical loads are carried by the module base. Horizontal seismic loads are carried to the module base through the plate diaphragms. The 10x10 modules are nominally 15' 2-3/4" high and 9' 1-1/2" square; the 10x11 modules are nominally 15' 2-3/4" high, 9' 1-1/2" wide and 10' 0" long. The modular base is approximately 1' 2-1/4" from the pool floor. The modules will be installed in the spent fuel pool which is 58' 6" long and 39' 3" wide.

The detailed design of the spent fuel storage cells is slightly different from the design for the Salem Nuclear Generating Station. Their basic function and construction, however, are similar. Figure 1-3 illustrates the storage cell design for the Donald C. Cook Plant. Each cell is a square cross-section formed from an inner shroud of stainless steel, a center sheet of aluminum clad B_4C, and an outer shroud of stainless steel. This cell acts as a storage space and, in addition, provides sufficient neutron absorption by the boron carbide contained in the Boral sheet to allow spacing of spent fuel in a 10.5 inch by 10.5 inch array. The fuel weight is carried directly on the module base. A flared guide and transition section is provided at the top of each storage cell. This transition is designed to assure ease of entry and to preclude fuel assembly hang-up and damage.

1.3 Specific Needs

Indiana & Michigan Power has a contract with Allied-General Nuclear Services (AGNS) for fuel reprocessing services. Currently, however, no spent fuel can be sent to AGNS for reprocessing due to the December 23, 1977 NRC order terminating licensing proceedings for the Barnwell facility.

Presently, there are 129 spent fuel assemblies stored in the spent fuel pool. Sixty-five assemblies were discharged from Unit No. 1 in January, 1977. The remaining sixty-four assemblies were discharged in April, 1978. One hundred and twelve burnable poison clusters are contained in these assemblies and an additional thirty burnable poison clusters occupy storage locations.

The total storage capacity expected to be utilized is based on maintaining a full core discharge reserve storage capability. The estimated refueling schedules and expected number of fuel assemblies to be transferred into the spent fuel pool are given in Table 1-1. From this table, it can be seen that the existing storage capacity would be filled by May, 1980 with FCDR.

* Trademark of Brooks and Perkins Incorporated

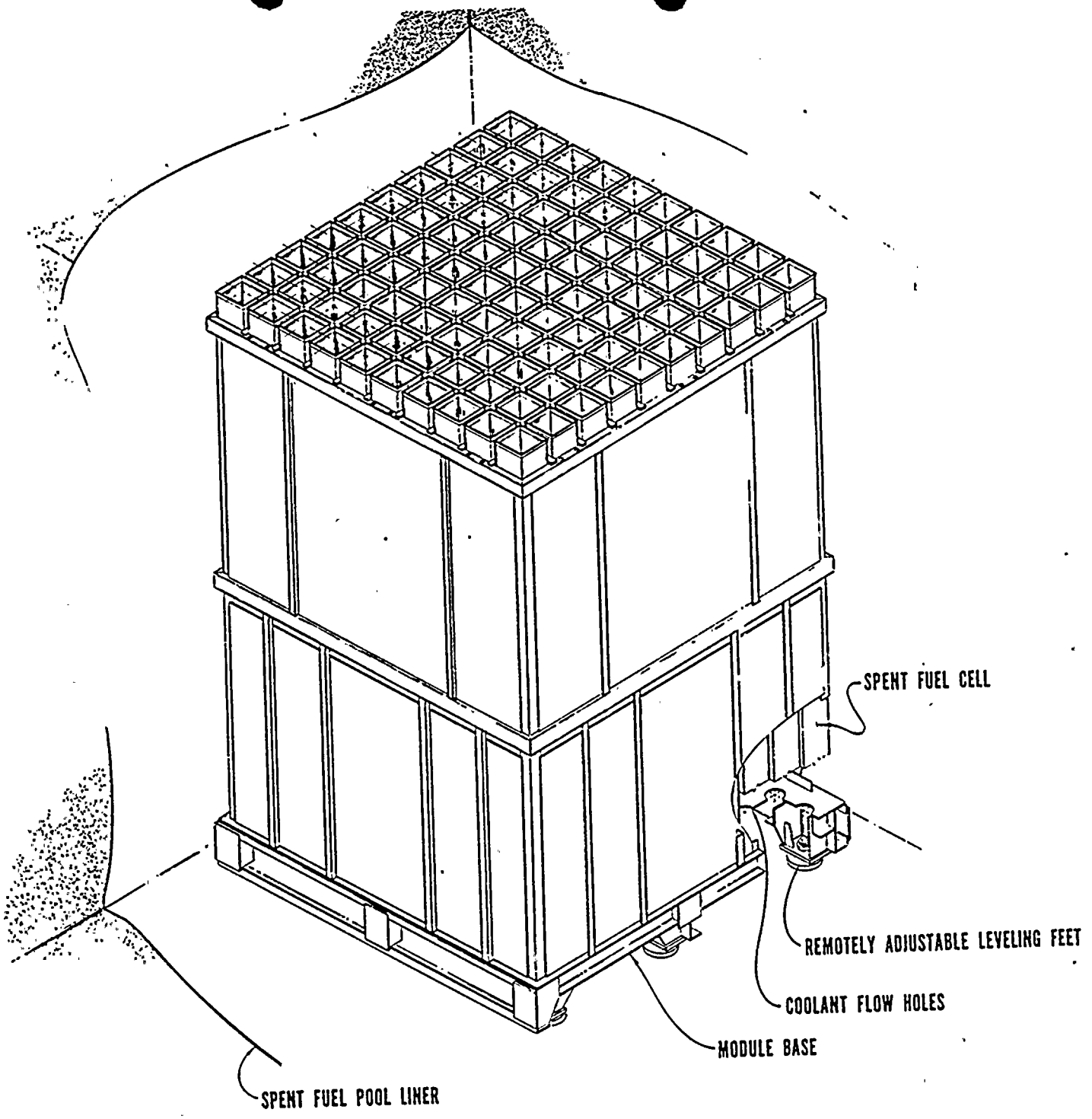

Figure 1.2
TYPICAL
HIGH-DENSITY POISON
SPENT FUEL STORAGE MODULE
10x10 ARRAY

9 MARCH 1979 sth

ATTACHMENT 3

Insert the attached page 3 and Table 3.5-1 and delete the similarly numbered ones from Attachment 1 to our transmittal No: AEP:NRC:00116 dated January 22, 1979.

3.5.1 Continued

Results

Thermal-hydraulic analysis of the natural convection cooling of a single fuel assembly indicates that there is adequate cooling under normal and even under hypothetical conditions where a loss of forced coolant circulation is assumed to occur. This result is based on the two (2) cases presented in Table 3.5-1. The table results are for the fuel storage cell located at the pool center as shown in Figure 3.5-1 and are therefore the worst case.

The first case is the normal situation where the heat generation rate is 54.1 kW per assembly and the fuel storage cell inlet temperature is taken as 150°F, the maximum expected pool operating temperature under normal conditions. The fuel rod peak cladding temperature is 190.0°F; therefore, there can be no boiling within the fuel assembly and the flow is single phase. 1

The second case is similar to the first except for the assumed inlet temperature, 240°F. This is the saturation temperature corresponding to the hydrostatic pressure at the top of the fuel storage cell. This is the maximum temperature that water flowing towards the fuel assembly inlet can attain under the hypothetical conditions where forced coolant circulation is assumed lost--and the surface of the pool is assumed to reach 212°F which is the saturation condition at that location. Under these assumed conditions, boiling does occur in the upper portion of the fuel assembly. Maximum cladding temperature under this case is calculated to be less than 250°F.

In summary, the analysis indicates that even under hypothetical extreme conditions, peak clad temperatures are well below conditions where any degradation of the clad would occur.

3.5.2 Spent Fuel Cooling Capability

An evaluation has been performed to determine the capability of the spent fuel pool cooling system (SFPCS) for providing the cooling capacity required for both the annual discharge of 65 fuel assemblies from Unit 1 and 88 fuel assemblies from Unit 2 on a 1-½ year cycle. It has been determined that the existing SFPCS, with both cooling loops in operation, can provide all necessary cooling for the normal discharge of fuel in the modified storage capacity condition. However, the design criterion for the cooling system, as stated in the FSAR, is that each of the two independent cooling loops be capable of providing adequate heat removal capacity in the event one loop is out of service. That design criterion states that with a

TABLE 3.5-1

Thermal Hydraulic Parameters For 54.1 kW
Fuel Assembly Located at Pool Center in Width Direction

Flow Type System Parameter	Single Phase Case 1	Two Phase Case 2	
Cooling Loop Operational	Yes	No	
Fuel Assembly Heat Generation Rate, kW	54.1	54.1	
Fuel Assembly Coolant Bulk Inlet Temperature	150	240	
Fuel Assembly Coolant Bulk Discharge Temperature, °F*	180.2	240	1
Bundle Coolant Bulk Maximum Temperature, °F	180.2	243	
Fuel Rod Film Temperature Drop °F, Max.	9.8	4.4	
Fuel Rod Peak Cladding Temperature °F	190	247.4	
Equilibrium Quality*	0	.005	
Void Fraction*	0	.526	1

* At top of assembly.